Proceedings of the Tenth Pacific Conference on Earthquake Engineering
Building an Earthquake-Resilient Pacific
6-8 November 2015, Sydney, Australia

Experimental study of precast concrete coupled walls

Zhang Weijing, Jiang Xiaopeng

Laboratory of Earthquake Engineering and Structural Retrofit of Beijing, Beijing University of Technology, Beijing, China

Qian Jiaru

Qinghua University, Beijing, China

ABSTRACT:

To investigate the seismic behavior of assembled monolithic coupling beams, six two-story assembled monolithic coupled shear walls were tested under the combined action of constant axial and cyclic lateral loads. The specimens were classified into three groups, each group has the same dimension and the similar reinforcement, the differences between the two specimens in the same group lie in the connection mode among the window wall of the first floor, post-poured strip and the spandrel under the window of the second floor. One specimen adopts single row of grouted sleeves splices while another has no sleeves. The test results indicated that the failure mode of the six specimens were similar, the main damage was flexural mode of failure. The bearing capacity and stiffness of the two specimens in each group were basically the same, the ultimate drift ratios were greater than 1.1%. whether the assembled monolithic coupling beam adopts grouted sleeves splices or not, its seismic behavior satisfies the China code specifications. However the relative sliding of the spandrel under the window of the second floor and later-poured strip and the damage of concrete at the interface was more serious for the coupling beams without grouted sleeve connection.

1 INTRODUCTION

Structures use prefabricated shear walls that are connected by cast-in-place perpends, horizontal seam and cast-in-place reinforced concrete floor slab or superimposed concrete slab. The structure accords with the development trends of housing industrialization and has wide application prospect in China for its high degree of industrialization, fast construction speed and being good for energy conservation and environmental protection [1-2].

Previous experimental studies [3] indicated that the stresses of the longitudinal reinforcements can be transferred effectively by grouted sleeves at the bottom of prefabricated shear wall. The precast shear wall has good seismic performance and can be equated as cast-in-situ shear wall if the longitudinal reinforcements of boundary members are connected separately by grouted sleeves and the vertical distributed reinforcements are indirectly connected by a single row of grouted sleeves. In recent years, precast concrete buildings have been used for high-rise apartment structure in China; Figure 1 shows the exterior wall panels of single-story height. Coupling beam is the important energy-consuming component of coupled shear walls for its seismic performance concerns the seismic performance of the whole structure [4]. Until now, there are no experimental studies reported on the seismic performance of the coupling beam of assembly integrated shear wall structures. Based on the engineering background of actual residential building, this paper presents the experimental research on seismic performance of coupling beams of assembly integrated shear wall structure through quasi-static tests of six two-story precast coupled shear walls.

Fig.1 Precast panels utilized in apartment building

2 EXPERIMENTAL PROGRAM

2.1 Test specimens

There were six specimens, each specimen was two-story coupled shear wall which was composed of two pieces of precast walls with openings, post-poured strip, post-poured wall piers, post-poured top beam and precast foundation. The story height of each specimen was 2900 mm, the total height was 6020mm above the foundation, the thickness of the wall was 200 mm, the height of window wall of the first floor and post-poured strip was 250 mm and the height of the spandrel under the window of the second floor was 800 mm, coupling beam of the first floor was composed of three sections, such as the window wall of the first floor, post-poured strip and the spandrel under the window of the second floor, these were the same as the actual engineering. The specimen size is shown in Figure 2.

According to variable parameters, six specimens were divided into three groups, the span-depth ratio and reinforcement of coupling beams of the first floor of the two specimens in each group were same, the difference between them lied in whether there were grouted sleeves splices between the vertical reinforcements of later-poured strip and the spandrel under the window of the second floor. Main parameters of specimens are given in Table 1.

Table 1 Main parameter of specimens

Group number	Specimen number	Height of the spandrel under the window of the second floor(mm)	Height of coupling beam (mm)	Span of coupling beam(mm)	Span-depth ratio of coupling beam	Connection mode
1	A	800	1300	2400	1.85	grouted sleeves
	B	800	1300	2400		no sleeves
2	C1	500	1000	1500	1.5	grouted sleeves
	D1	500	1000	1500		no sleeves
3	C3	500	1000	2400	2.4	grouted sleeves
	D3	500	1000	2400		no sleeves

In order to make sure that the coupling beam of the first floor damaged at first, wall piers and the coupling beam of the second floor were strengthened, the coupling beam of the first floor was weakened. The reinforcement details of specimen A are shown in Fig.2; the reinforcements in other specimens were similar. Hot-rolled ribbed steel bars were used for longitudinal and transverse reinforcement of the specimens, which has yield strength of 400Mpa (named HRB400). There were six 16 mm-diameter vertical bars in each wall pier of precast walls, four 16 mm-diameter horizontal bars in precast beam of the first floor, four 16 mm-diameter, four 10 mm-diameter and four 8 mm-diameter horizontal bars in the precast beam below the window of the second floor, three 25 mm-

diameter and two 16 mm-diameter horizontal bars in the precast beam below the post-cast top beam. There were ten 18 mm-diameter vertical bars in the cast-in-situ wall pier, four 16 mm-diameter horizontal bars in the post-poured strip of the first floor, four 16 mm-diameter and three 25 mm-diameter horizontal bars in the post-poured top beam of the second floor. Transverse reinforcement consisted of hoops made from 8 mm or 10 mm diameter spaced at 150 mm or 200 mm.

8 mm-diameter U-shaped stirrups spaced at 200mm was adopted between the precast window wall of the second floor and post-poured top beam, the precast window wall of the first floor and post-poured strip. As for the former specimen of each group, single row of sleeves at the spacing of 400mm were provided at the bottom of the spandrel below the window of the second floor. The vertical reinforcements of the spandrel below the window of the second floor were connected with the end of sleeves with threads; the vertical reinforcements pre-embedded in the window wall of the first floor were inserted into the sleeve through post-poured strip. Grouting material was poured into sleeves and the diameter of reinforcement in the sleeve was 16 mm.

10 mm-diameter U-shaped stirrups spaced at 200mm were adopted between the precast wall and post-poured wall piers. The vertical reinforcements at the bottom of post-poured wall piers lapped with the vertical reinforcements reserved in the foundation. The splicing of two rows of twelve 16 mm-diameter bars grouted sleeves was adopted between the precast wall piers of the first floor and the second floor. The same splicing was adopted between the precast wall piers of the first floor and the foundation, the connection between the post-poured wall piers of the first floor and the foundation was changed into steel plate welding.

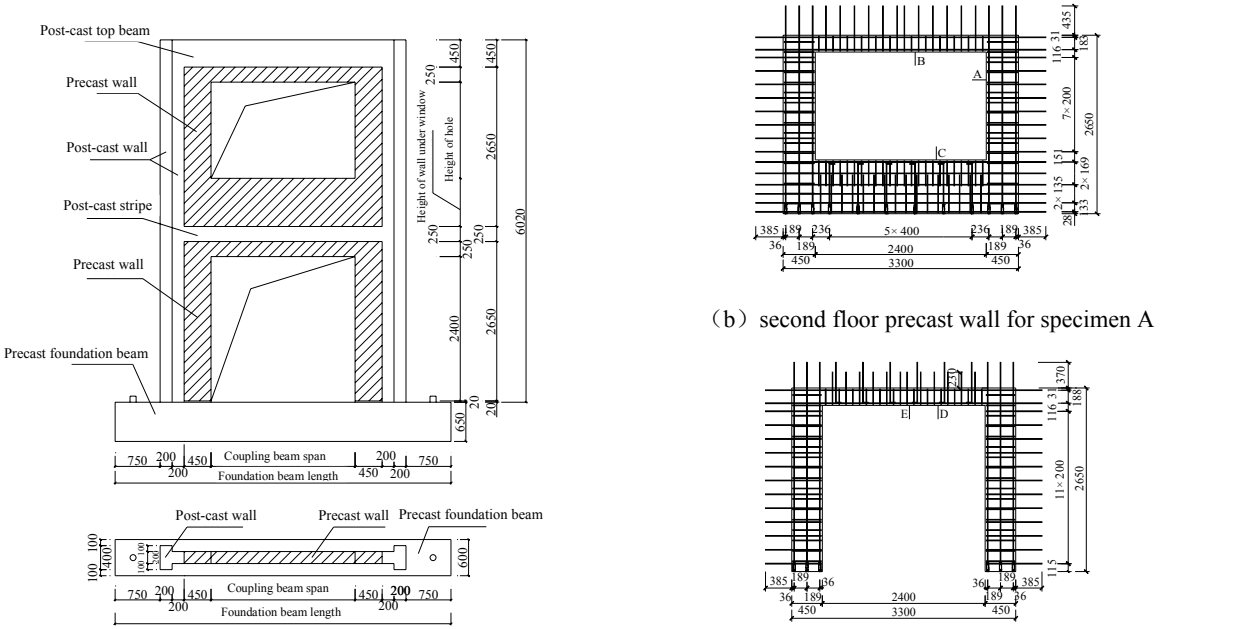

（a）specimen dimensions

（b）second floor precast wall for specimen A

（c）first floor precast wall for specimen A

Fig.2 Specimen dimensions and reinforcing details for specimen A

2.2 **Material properties**

The material of reinforcements in all specimens adopted HRB400 steel as the same as the practical engineering. The design strength grade of concrete was C40. The measured cube compressive strength of concrete f_{cu} of the specimens A1, B1, C1, D1, C3, D3 were 65.5MPa, 68.9MPa, 57.6MPa, 59.9MPa, 66.2MPa, 59.7MPa, respectively, the axial compressive strength of concrete f_c was taken to $0.76f_{cu}$. The mechanical properties of reinforcement are shown in Table 2, the elasticity modulus E_s of all rebars is 2.0×10^5 MPa and the yield strain ε_y is calculated as the yield Strength f_y divided by E_s.

Table 2 Mechanical properties of reinforcement

Steel Label	f_y* [MPa]	f_u* [MPa]	ε_y*
Φ8	407.8	580.9	2039×10^{-6}
Φ10	445.6	532.2	2228×10^{-6}
Φ12	434.2	541.3	2171×10^{-6}
Φ16	441.2	598.6	2206×10^{-6}
Φ25	484.8	611.2	2424×10^{-6}

* f_y is the yield strength; f_u is the ultimate strength; ε_y is the yield strain.

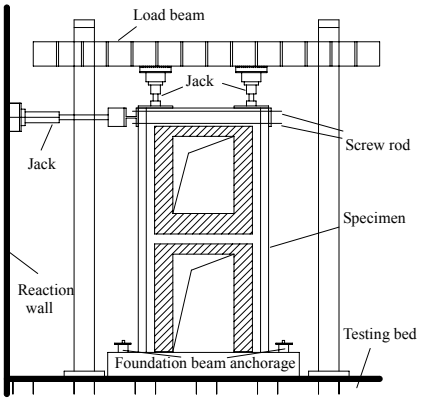

Fig. 3 Test setup

2.3 **Test setup and instrumentation**

The precast coupled walls were tested under the combined action of constant axial and cyclic lateral loads. The test setup and instrumentation is shown in Figure 3. All the specimens were fixed to pedestal by foundations. Two 500kN axial load was exerted by a pair of servo-controlled hydraulic jacks with 600kN capacity; cyclic lateral load (displacement) was exerted by a hydraulic jack with 1000kN capacity and its axis is 5795mm distant from the top of foundation.

Displacement control method was adopted as the loading rule and the displacement is measured by linear variable displacement transducer which is 5470mm above the top of foundation. Pushing and then pulling are respectively named as positive loading and reverse loading. The first three drift ratio levels are 1/2000、1/1000 and 1/750, one cycle for each level; after the 1/500 drift level, the application of lateral displacement were followed by cycles with increments of 10mm until the end of tests, each cycle of this phase was repeated two times.

To monitor required displacements, six LVDTs (linear variable transducers) were mounted on the required points of the specimens. In addition to the LVDTs, a number of strain gauges were mounted on certain longitudinal and transverse reinforcement in the beams. The applied lateral loads were measured using the actuator load cell.

3 **EXPERIMENTAL RESULTS**

3.1 **Cracking Patterns**

Take the specimen A as an example, the failure process of the specimen is introduced. Initial cracking was characterized by the formation of hairline vertical cracks at the ends of the coupling beam, then these cracks became more inclined as they extended into beam. At the drift ratio of 0.2%, vertical cracks went through the height of the beam, and some horizontal cracks up to 10mm long were observed. At the drift ratio of 0.5%, part of cracks in coupling beam developed along the 45 degree and formed corner to corner diagonal cracks；Short horizontal cracks occurred at the bottom of mid portion of coupling beam；horizontal cracks also occurred in the wall piers，the concrete cover at the base of piers started to spall due to compression. At the drift ratio of 0.7%, minor horizontal cracks were observed at the intersection of spandrel and post-poured strip. At the drift ratio of 0.9%, cracks became wider at the corner of the coupling beam, concrete started to spall and a small amount of reinforcements were exposed. The horizontal cracks at the intersection of spandrel and post-poured strip developed and became wider. At the drift ratio of 1.1%, the horizontal cracks at the intersection of spandrel and post-poured strip went through the length of coupling beam. At the drift ratio of 1.2%, the width of some cracks at the corner of coupling beam was up to 10mm, crushing of concrete at corner of coupling beam and buckling of reinforcement occurred, and extensive spalling is observed. At the drift ratio of 1.6%, spalling of concrete cover became severe at the intersection of spandrel and post-poured strip. At the drift ratio of 1.8%, longitudinal and transverse reinforcements were exposed, buckling of longitudinal reinforcement was obvious.

All the specimens failed in an approximately similar way. The cracking of concrete occurred at the

ends of coupling beams, the reinforcement of this area have severely buckled. The spalling of concrete cover occurred. Horizontal cracks between the post-poured strip of the coupling beam and the spandrel under the window of the second floor were obvious due to relative sliding. By comparison the specimens of the same group, the coupling beam without grouted sleeves failed more seriously than that of with grouted sleeves. The photos of specimen after failure are shown in Figure 4.

（a）Specimen A

（d）Coupling beam of Specimen A

（e）Coupling beam of Specimen B

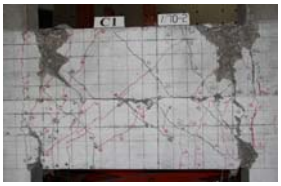

（f）Coupling beam of Specimen C1

（g）Coupling beam of Specimen D1

（b）Left corner of coupling beam for Specimen A

（c）Right corner of wall pier for Specimen A

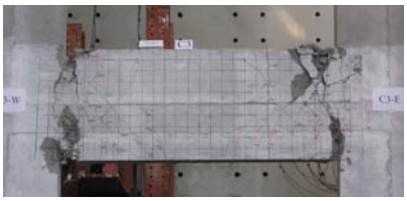

（h）Coupling beam of Specimen C3

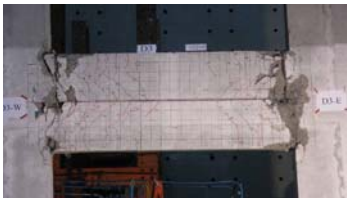

（i）Coupling beam of Specimen D3

Fig.4 Specimen photos after failure

3.2 **Lateral load-deformation response**

The lateral force- top displacement of all specimens is shown in Figure 5, and the lateral force- first floor displacement of all specimens is shown in Figure 6.

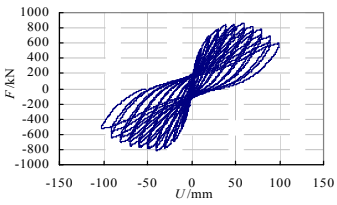

（a）Specimen A

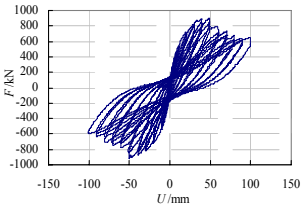

（b）Specimen B

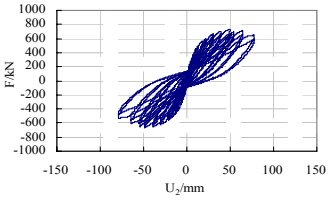

（c）Specimen C1

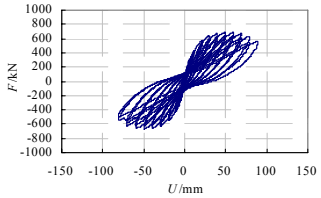

（d）Specimen D1

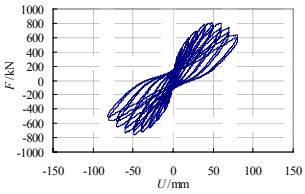

（e）Specimen C3

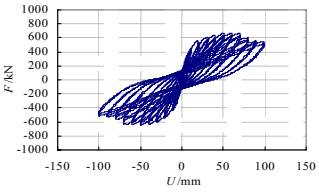

（f）Specimen D3

Fig.5 Lateral load versus top displacement relations

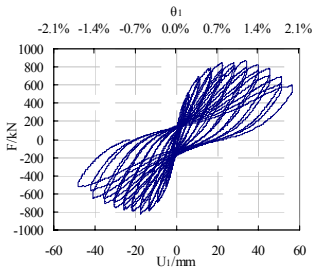

（a）Specimen A

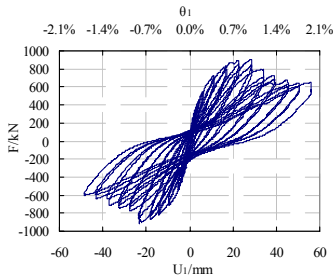

（b）Specimen B

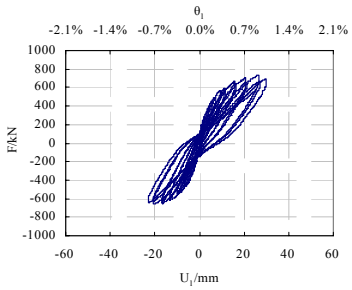

（c）Specimen C1

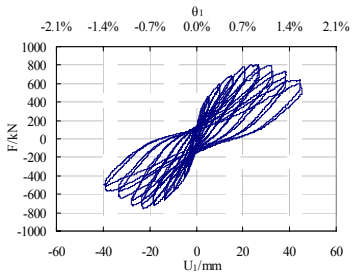

（d）Specimen D1

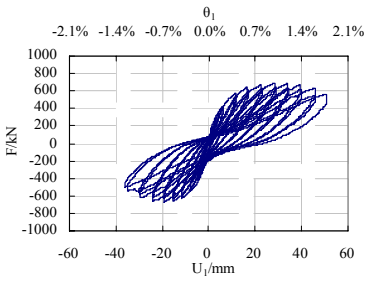

（e）Specimen C3

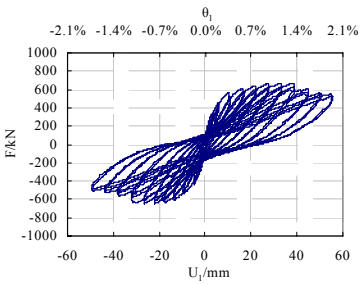

（f）Specimen D3

Fig.6 Lateral load versus first floor displacement relations

It is clear from the Figure 5 and Figure 6 that no obvious pinching occurred, showing that the specimens have good energy dissipation capacity.

Skeleton curves of lateral force-top displacement is shown in Figure 7. It can be seen that after the peak lateral force, the bearing capacity of each specimen decrease slowly, showing good ductility. Comparison of the specimens in the same group (A and B, C1 and D1), skeleton curve is almost identical before yielding, the initial stiffness is same; the lateral loading of the specimen with sleeves is slightly lower than that of without sleeves after yield to peak. For the third group specimens with span to depth ratio 2.4, the backbone curves are basically coincident.

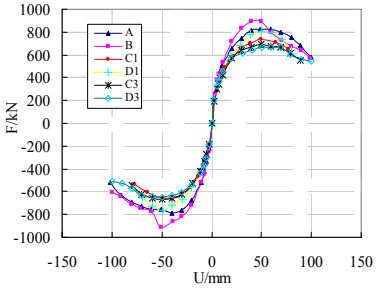

Fig.7 Skeleton curves

3.3 **Bearing capacity**

Table 3 shows the average values of cracking strength F_c , nominal yield strength F_y and the peak strength F_p. It can be seen that the two specimens in the same group have similar cracking load，nominal yield load and peak load. Whether the use of sleeve connection between the window wall and post pouring strip have little effect on the bearing capacity.

Table 3 Cracking load F_c , nominal yield load F_y and the peak load F_p

Group number	First		Second		Third	
Specimen number	A	B	C1	D1	C3	D3
F_c/kN	278.4	308.8	288.2	204.5	239.1	315.3
F_y/kN	583.8	644.5	501.8	535.5	490.0	482.6
F_p/kN	818.2	905.0	697.3	781.5	678.4	657.0

3.4 **Deformation capacity**

Define first floor drift ratio $\theta_1 = U_1 / h_1$, where U_1 is the lateral displacement measured at first floor, h_1

is the height of measured point, taken as 2800 mm. Ductility factor of first floor is calculated by μ_{1u} $=U_{1u}/U_{1y}$, where U_{1y} is the lateral displacement responding to the yield load, U_{1u} is the lateral displacement responding to the ultimate load. Define the ultimate point is the 85% of peak lateral load.

Table 4 shows the average value of cracking displacement U_{1c} （drift θ_{1c}）, nominal yield displacement U_{1y} （drift θ_{1y}）, the peak displacement U_{1p}（drift θ_{1p}）, the ultimate displacement U_{1u} （drift θ_{1u}） and the deformation ductility μ_{1u}. The results show that the two specimens in the same group have similar nominal yield displacement, the peak displacement and the ultimate displacement （except the first group）. Whether in use grouted connection between the window wall and post pouring strip have little effect on the deformation of specimen. The average value of peak displacement is greater than the drift limit value of 0.8% which required by the China's code for the shear walls under severe earthquake, the average value of ultimate drift is greater than 1.1%.

Table 4 Drift ratio at different levels for first floor

Group	First group		Second group		Third group	
Specimen	A	B	C1	D1	C3	D3
U_{1c}/mm (θ_{1c})	2.5 (0.09%)	3.0 (0.11%)	2.7 (0.1%)	1.4(0.05%)	1.5(0.05%)	2.5(0.09%)
U_{1y}/mm (θ_{1y})	7.5 (0.27%)	8.5 (0.3%)	7.0 (0.25%)	8.1(0.29%)	7.5(0.27%)	7.1(0.26%)
U_{1p}/mm (θ_{1p})	29.7(1.1%)	25.9(0.93%)	23.8 (0.85%)	27.7(1%)	26.7(0.95%)	30.4(1.1%)
U_{1u}/mm (θ_{1u})	43.1(1.54%)	30.9(1.1%)	31.9 (1.14%)	37.5(1.34%)	40.5(1.45%)	44.1(1.57%)
μ_{1u}	5.7	3.6	5.0	4.6	5.4	6.2

3.5 **Shear deformation of coupling beam**

The measured deformation $\overline{X}$ and shear stress γ are listed in Table 5. The results show that the shear deformation is similar for the two specimens in the same group.

Table 5 Shear deformation

Group number		First		Second		Third	
Specimen ID		A	B	C1	D1	C3	D3
direction		positive negative	positive negative	positive negative	positive negative	positive negative	positive negative
cracking	$\overline{X}$ (mm)	0.27 0.01	0.63 0.62	0.46 0.42	0.23 0.20	0.53 0.23	0.85 0.48
	γ (×10-3)	0.23 0.01	0.55 0.54	0.55 0.51	0.27 0.24	0.57 0.24	0.92 0.52
yield	$\overline{X}$ (mm)	1.44 1.67	2.40 2.16	2.14 1.99	2.41 1.90	2.07 2.96	2.17 2.84
	γ (×10-3)	1.26 1.46	2.10 1.89	2.58 2.40	2.90 2.28	2.24 3.20	2.35 3.08
peak	$\overline{X}$ (mm)	9.05 10.52	8.06 10.18	8.72 8.26	6.70 5.43	7.82	11.44 10.48
	γ (×10-3)	7.92 9.21	7.05 8.91	10.48 9.93	8.05 6.52	8.47	12.39 11.35
ultimate	$\overline{X}$ (mm)	16.85 27.27	—	32.60 20.34	15.56 22.65	—	22.5 18.76
	γ (×10-3)	14.74 23.86	—	39.18 24.44	18.70 27.23	—	24.37 20.3

3.6 **Stiffness**

Equivalent stiffness was defined as secant stiffness corresponding the maximum displacement for each cycle. A plot showing the reduction in equivalent stiffness with deformation amplitude for all specimens is shown in Figure 7. The results show that the stiffness curves are coincident for the same group specimens before yielding. After that and before ultimate displacement, the stiffness of the

specimen without grouted sleeves is greater than that of specimen with sleeves. At the 90mm displacement level, the stiffness degradation of all specimens is similar.

The measured cracking equivalent stiffness, yield equivalent stiffness, peak equivalent stiffness, and ultimate equivalent stiffness are listed in Table 6. By comparing the specimens in same group, Whether the use of sleeve connection between the window wall and post pouring strip have little effect on the stiffness. By comparing the specimens of different groups, the specimen in first group is a little greater than that of the other two groups. When the lateral load reaching the peak, the equivalent stiffness decreased to 40% of the yield stiffness. The specimen has enough stiffness to resist deformation after yielding, which is helpful for the safety redundancy of the specimen.

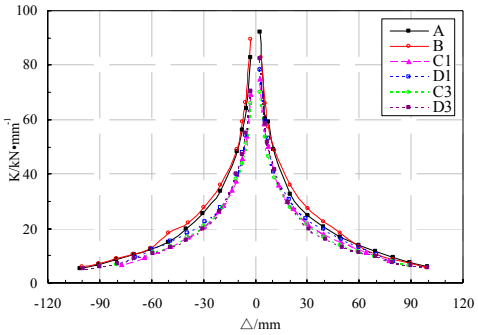

Fig.7 Stiffness deterioration curves for specimens

Table 6 Equivalent stiffness of specimen （kN/mm）

Group number	First		Second		Third	
Specimen ID	A	B	C1	D1	C3	D3
K_{cr}	66.3	65.7	55.4	73.0	56.9	57.3
K_y	39.2	39.5	33.0	30.4	30.2	33.1
K_p	16.5	18.2	14.2	15.8	13.8	11.0
K_u	8.1	12.3	8.1	9.1	7.2	6.4

4 CONCLUSIONS

Based on the experimental research on two-story precast concrete coupled walls, the following findings are summarized as follows:

(1) The failure mode are similar: the plastic hinge formed at the ends of the coupling beam. the crushing of concrete was observed at the base of wall piers. The horizontal cracks occurred at the interface of the post-poured strip and the spandrel under the window of the second floor due to relative sliding.

(2) Hysteretic curves of all specimens are more full. For the first two group specimens with the same span-depth ratio, skeleton curves are coincident before yielding, and the initial stiffness are almost the same. The lateral loading of the specimen with grouted sleeves is slightly lower than that of without grouted sleeves after yield to the peak. For the specimen C3 and D3 with span to depth ratio 2.4, the skeleton curves are basically coincident.

(3) Whether the use of sleeve connection between the window wall and post pouring belt had little effect on the load capacity, deformation and stiffness of specimens. At the nominal yield and peak level, the shear deformation of coupling beam had little difference whether the sleeve connection are provided or not.

(4) The average values of ultimate drift ratio is greater than 1.1%, which satisfied the limit value of the inter story drift for the shear walls under severe earthquake. The deformation capacity of coupling beams satisfy the requirements of the deformation capacity of shear wall structure under strong earthquake.

(5) Before reaching the peak capacity, most longitudinal reinforcement yielded at the top and bottom of the coupling beam, while the transverse reinforcement didn’t yield. At the stage of bearing capacity decline, part of transverse reinforcement yielded.

(6) With the increasing of the relative stiffness of coupling beam, the integral stiffness and bearing capacity increased, however, the deformation and ductility capacity decreased.

AKCNOWLEDGEMENT

The work presented in this paper was supported by funds from Beijing Municipal Natural Science Foundation under Grant No 8152010, Key Laboratory of Urban Security and Disaster Engineering, Ministry of Education and Key Laboratory of Earthquake Engineering and Structural Retrofit of Beijing under Grant No USDE201402. These financial supports are gratefully acknowledged. The authors would like to thank Prof. Wallace, the director at UCLA, for his opinion on the project.

REFERENCES:

Wang D., and Lu X.L. 2010. Progress of study on seismic performance of precast concrete shear wall systems. *Structural Engineers*. 26(6):128-135. (in Chinese)

Chen T., Guo H.Q., Ma T., et al. 2011. Engineering application on housing industrialization of precast reinforced concrete shear wall structure [J]. *Building Structure*. 41 (2): 29-30. (in Chinese)

Qian J.R., Peng Y. Y., and Zhang J.M. 2011.The seismic performance experiment of vertical reinforcements spliced by grout sleeves precast concrete shear wall [J]. *Building Structure*. 41, (2) : 1-6. (in Chinese)

Brena.S.F. and Ihtiyar.O. 2011. Performance of conventionally reinforced coupling beams subjected to cyclic loading. *J. Struct. Eng*., 137(6), 665-676

GB50010-2010, Code for seismic design of buildings [S]. Beiing: *China Architecture & Building Press*, 2010. (in Chinese)

JGJ101—96, Specification of testing methods for earthquake resistant building [S]. Beiing: *China Architecture & Building Press*, 1996. (in Chinese)